AsPac J. Mol. Biol. Biotechnol. 2024
Vol. 32 (3) : 128-146

Surface functionalization of oil palm empty fruit bunch (OPEFB)-derived cellulose as a carboxyl platform for metal cations and dyes removal from aquatic media

Noerhidajat Sjahro[a], Robiah Yunus[a,b*], Luqman Chuah Abdullah[a], Suraya Abdul Rashid[a,c], Ahmad Jaril Asis[d], Dina Kania[b], Alsultan Karim[c]

[a]*Dept. Chemical and Environmental Engineering, Faculty of Engineering, UPM, Selangor, Malaysia*
[b]*Institute of Plantation Studies, UPM, Selangor Malaysia*
[c]*Institute of Nanotechnology and Nanoscience, Universiti Putra Malaysia, Selangor, Malaysia*
[d]*Sime Darby Plantation Sdn. Bhd., Malaysia*

Received 16th March 2024 / Accepted 3rd July 2024 / Published 14th August 2024

Abstract. The abundant oil palm empty fruit bunch (OPEFB) as by-product of palm oil milling processes exhibits a potential as an alternative cellulose feedstock for bio-adsorbent. This study aimed to produce a highly carboxylated bio-adsorbent for direct industrial application from OPEFB-based cellulose via mercerization and followed by esterification with succinic anhydride (SA) to enhance its adsorptive capability towards hazardous heavy metal and dyes ions. The modification using SA provides the carbon backbone platform for carboxyl group attachment for the contaminants. The results showed that the carboxylated cellulose had a high carboxyl content (4.39 mmol/g). Carboxylated cellulose had a higher binding capacity for adsorbates, with removal rates of 94.7%, 97.85%, 40.9%, and 90.15% for dye, Pb^{2+}, Cu^{2+}, and Cd^{2+} cations, respectively, at pH 6, 4 hours reaction time, and at room temperature. In comparison, unmodified cellulose removed only 47%, 23.1%, 2.9%, and 7.5% for dye, Pb^{2+}, Cu^{2+}, and Cd^{2+} cations, respectively. The adsorption kinetics study revealed that the adsorption process followed the pseudo-second-order model. The adsorption isotherm of these two metal cations follows the model of Langmuir very well, while Cu^{2+} follows the Freundlich model. Our method produces bio-adsorbents with high carboxyl content and adsorption rate in a short reaction time using OPEFB as a green precursor material that is easily scalable for industrial use.

Keywords: aquatic contaminants, carboxylation, carboxyl group-platform, OPEFB cellulose

INTRODUCTION

Heavy metals and dyes are hazardous contaminants originating primarily from industrial wastewater and effluents that have caused a severe global environmental problem (Le & Nunes, 2016). Heavy metals, such as lead, cadmium, chrome, and mercury are toxic even at low concentrations (Rahman & Singh, 2019), while dyes are thermally and chemically stable, posing adverse risks to living organisms and environment (León *et al.*, 2018). Industrial dyes are generally classified into two categories, i.e., ionic (anionic and cationic) and nonionic. This issue has prompted intensive research into new advanced treatment technologies, some of which are currently being implemented on a large scale. Among the technologies, adsorption is considered one of the most effective, practical, and inexpensive methods for removing metal and dyes from industrial wastewater (de Gisi et al., 2016; Song et al., 2020a). The adsorption method in water treatment has several advantages for it has high efficiency, simple operation, and associated with non-toxic properties (Sefid Siahbandi *et al.*, 2023). The removal of dyes from industrial

*Author for correspondence: Professor Dr. Ir. Robiah Yunus, Department of Chemical and Environmental Engineering, Faculty of Engineering, UPM, Serdang Malaysia 43400
Email – robiah@upm.edu.my

wastewater has been done by various methods, such as chemical, ultrafiltration, ion exchange, reverse osmosis, and adsorption using different adsorbents, for instance, using activated carbon, zeolite, silica gel, and photocatalysis. The mechanism of adsorption is enabled through π- π bonding, hydrogen bonding, and electrostatic interaction (Moradi *et al.*, 2022), Donnan effect, ion exchange, and surface complexation (Chong *et al.*, 2019). The solution pH is one of the most important factors in the adsorption process that can change the surface charge of adsorbents as well as the separation of functional groups in the active sites of the adsorbent.

Recently, cellulose materials as green precursors are gaining much attention for their potential use as renewable, biodegradable, and biocompatible biomass adsorbents (Bhadoria *et al.*, 2022; Daneshfozoun *et al.*, 2014; Fan *et al.*, 2019; Song *et al.*, 2020; Wong *et al.*, 2020; Zhou *et al.*, 2020). Cellulose is the most abundant organic polymer on earth and a major component of plant cell walls with a polysaccharide structure similar to starch (Sun *et al.*, 2016). Cellulose can be produced from a wide variety of plants and trees since it is one of lignocellulosic constituents, primary building block of plants. In 2017, 69.87 million tons of oil palm empty fruit bunches (OPEFB) were generated as a byproduct of palm oil extraction, necessitating the conversion of this biomass into valuable products (May *et al.*, 2019). The OPEFB fiber contains around 35 – 65% cellulose by mass (Ching & Ng, 2014; Lee *et al.*, 2014) or 40% by weight on average (Awalludin *et al.*, 2015), making OPEFB the most potential source of cellulose.

Despite being abundant, the use of unmodified OPEFB as an adsorbent exhibited a low adsorption capacity. Another factor to consider is the extraction method used to separate cellulose from other lignocellulosic constituents and remove impurities. Naturally, these biopolymers are present in terrestrial plants and algae as cell walls constituent alongside tightly intertwining hemicellulose and lignin. The presence of lignin and cellulose crystallinity causes its recalcitrant nature to chemical modifications (Yang *et al.*, 2019). In addition, cellulose-based adsorbent with three native hydroxyls attached to each glucose carbon backbone has a poor binding and low ion-exchange capacity for metals (Suhas *et al.*, 2016).

However, cellulose adsorption performance can be significantly enhanced through modification (Daneshfozoun *et al.*, 2017; Asadpour *et al.*, 2021; Septevani *et al.*, 2020) of its hydroxyl functional groups. Oxidation, etherification, esterification, carboxylation, sulfonation, silylation, and polymer grafting are among the chemical functionalization reactions that can introduce some groups with the capacity of chelating metals to the cellulose surface, such as carboxyl and amine groups (Fan *et al.*, 2019; Gago *et al.*, 2020; Kassab *et al.*, 2019; Leszczyńska *et al.*, 2019; Sjahro *et al.*, 2021). The modification mainly substitutes the rich content of hydroxyl groups on the cellulose surface with other functional groups, tailored to achieve favorable conditions for water and wastewater treatment.

Among common derivatives, carboxylated cellulose (cell-COOH), for instance, has excellent adsorption performance compared to its native functional groups. Previous studies synthesized carboxylated cellulose from various precursor materials, such as commercial microcrystalline cellulose (Fan *et al.*, 2019; Leszczyńska *et al.*, 2019), commercial cellulose (Gago *et al.*, 2020), or Juncus plant (Kassab *et al.*, 2020). Periodate−chlorite oxidation, citric acid mixtures, 2,2,6,6-tetramethylpiperidine-1-oxygen (TEMPO) oxidation, and ammonium persulfate (APS) oxidation are some popular protocols for the synthesis of carboxylated cellulose (Fan *et al.*, 2019). Gurgel *et al.* (2008) and Sehaqui *et al.* (2017) reported that the modified cellulose synthesized with succinic anhydride (SA) had a satisfactory high carboxyl content of 6.2 mmol/g and 3.8 mmol/g, respectively, compared to other reagents, such as Fe^{2+}/H_2O_2, maleic anhydride, and sodium 2-bromomalonate (BMA) (Fan *et al.*, 2019b; Qiao *et al.*, 2015a; Gago *et al.*, 2020b). Daneshfozoun *et al.* (2014) produced OPEFB-derived carboxylated cellulose adsorbent using acetic acid and ethylenediaminetetraacetic acid (EDTA, containing four carboxyl groups per molecule). However, the carboxyl content of modified cellulose has not been reported. Nevertheless, previous research focusing on the carboxylation of OPEFB-derived cellulose is still limited.

In this study, OPEFB-derived cellulose was chemically modified and tested for hazardous heavy metals and dye uptake. Succinic anhydride (SA) was used as a reagent to produce modified cellulose with high carboxyl content and excellent metal-chelation as a bio-adsorbent. The carboxylated cellulose performance in removing three heavy metal cations and dyes from an aqueous medium was tested, and the adsorption kinetics was studied. This method is scalable due to the short reaction time and the high yield of carboxylated cellulose obtained after surface modification. This study could also lead to new techniques to separate cellulose from other lignocellulosic constituents and remove impurities, thereby supporting the development of further industrial applications.

MATERIALS AND METHODS

Materials

Succinic anhydride (SA), NaOH, and $NaClO_2$ were obtained from R & M Chemicals Malaysia. All materials and reagents were used as received without further purification. Metal ions (Pb, Cu, and Cd) solutions were obtained from stock solution; $Pb(NO_3)_2$, $Cu(NO_3)_2$, and $Cd(NO_3)_2$ 10 M from Merck, Germany. Later, pH adjustment was made by adding HCl or NaOH to the stock solution. All chemicals were of reagent grade, and the solvents were of analytical grade. The raw oil palm empty fruit bunch (OPEFB) fiber was obtained from Sime Darby Plantation.

OPEFB cellulose isolation

OPEFB fiber was rinsed with tap water to remove debris, sand, and soil. The fibers were then manually chopped and ground into small-sized fibers, subsequently pretreated with NaOH 5% for an hour, bleached with $NaClO_2$ 5% for 2 h, and repeated twice. Next, the fibers were refluxed with HCl 2% for 2 hours and washed several times until neutral pH was reached. The obtained cellulose, $(C_6H_{10}O_5)_n$, was kept in an airtight container for further use.

Cellulose mercerization

Ground OPEFB cellulose (cellulose 1) (10 g) was immersed in 200 mL of NaOH solution (20 wt%) in a glass beaker at room temperature for at least 16 h with constant stirring. The alkali-cellulose was centrifuged to separate the supernatant and cellulose sediment and then washed with distilled water. Later, washing was continued with vacuum filtration using Whatman filter paper with distilled water to neutrality (pH 7). Finally, the mercerized product was dried at 90°C in an oven for 1 h and stored in a desiccator (Hokkanen *et al*., 2013).

Cellulose carboxylation with succinic anhydride (SA)

The protocol of carboxylation of cellulose was modified from Sehaqui *et al*. (2017) and Zhang *et al*. (2017), as depicted in Figure 1. Mercerized OPEFB cellulose was poured into a round bottom flask containing 0.75 g and 2.6 g of SA (7.4 and 26 mmol, respectively) was completely dissolved in the mixture of 26 mL dimethyl formamide (DMF) and 0.25 mL of pyridine, 1.2 g (7.4 mmol). The flask was heated at a constant temperature at 90°C for various durations of 1, 2, 3, and 4 h under magnetic stirring at 350 rpm in an oil bath. The ratio of SA to mercerized cellulose was 1.3 : 1. Subsequently, the suspension was cooled down in an ice bath for several minutes.

The OPEFB-derived cellulose was then thoroughly centrifuged and washed with distilled water and acetone, followed by drying at 80°C in an oven for 1 hour and overnight in a desiccator. Finally, the mixture was centrifuged again to separate the supernatant and sediment. The supernatant was discarded and the sediment was vacuum filtered several times with distilled water and finally with hot water to remove any residual DMF and SA, as indicated by the rinsing water reaching a neutral pH. The carboxylated cellulose was then oven-dried at 70°C until it reached a constant weight. Later, the dried cellulose was ground into powder for analysis and batch adsorption testing.

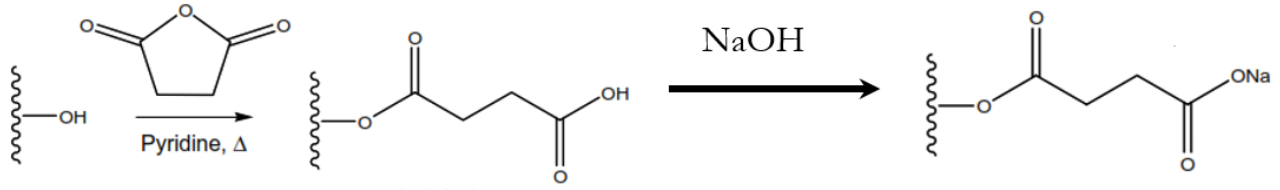

Figure 1. Cellulose modification using succinic anhydride (SA) (Gurgel *et al.,* 2008)

Characterization of carboxylated cellulose adsorbent

Characterization of modified cellulose after carboxylation using SA was performed to determine the content of carboxylate groups successfully introduced into the cellulose surface. Fourier transform infrared (FTIR) analysis was performed first to ensure chemical structure on the surface. In addition, the cellulose crystallinity and morphological structure were also determined using X-Ray diffraction (XRD) analysis and scanning electron microscope (SEM) image analysis.

FTIR analysis

FTIR analysis was performed using infrared spectrophotometer (Thermo Scientific, model Nicolet Nexus 6700) to determine the chemical properties of the sample, such as functional groups, molecular fingerprints, and chemical sample composition, as well as the success of the esterification reaction. The spectra of all samples were measured in the range of wavenumber from 650 to 4,000 cm^{-1} and the corresponding transmittance was also recorded.

SEM analysis

Morphological characterization of the samples was performed using an SEM (Hitachi, model S3400N). The scan images were acquired with a magnification of 150 – 500× and an accelerating voltage of 10 – 15kV. Prior to morphological assessment, the samples were mounted on an aluminum stub and sputter-coated with Au-Pd to ensure the high quality of the scan images.

XRD analysis

The crystallinity index of a sample was determined using XRD with the following measurement details: X-ray tube target Cu, voltage 40.0 (kV), current 30.0 (mA), use of divergence slits of 1.00000 (deg), scatter slit 1.00000 (deg), and receiving slit 20.000 (mm). Meanwhile, the scan conditions were set as follows: drive axis 2 Theta, scanning range from 5,000 to 80,000, continuous scanning mode, speed of 5,0000 (deg/min), sampling pitch 0.0200 (deg) and present time 0.60 (sec). The crystalline index of the modified cellulose was determined using Segal's empirical equation as follows:

$$CI(\%) = \frac{I(22^o) - I(18^o)}{I(22^o)} \qquad \text{(Eq. 1)}$$

Where CI refers to the crystallinity index of modified cellulose, I(22°) represents the peak diffraction intensity corresponding to crystalline cellulose, I(18°) denotes the peak diffraction intensity, corresponding to the amorphous regions of cellulose at 2θ and equal to 22° and 18° (Liu *et al.*, 2014).

Determination of carboxyl group content

The content of carboxyl group (COOH) in the cellulose was determined using the retro titration method. After drying and grinding, 0.25 – 0.5 g of the modified cellulose was poured into a 50 -100 mL 0.01 M solution of NaOH. The suspension was stirred sufficiently with magnetic stirring for an hour at 500 rpm. Several drops of phenolphthalein were added as a basic indicator until the mixture turned pink. The suspension was then titrated with 0.1 M HCl solution using a burette until the solution reached neutrality, indicating a color change from pink to clear. The COOH content (in mmol/g) of the suspension containing carboxylated cellulose was determined using Eq. 2.

$$C_{COOH} = \frac{(C_{NaOH}.V_{NaOH}) - (C_{HCl}.V_{HCl})}{m_{cell}} \qquad \text{(Eq. 2)}$$

Where C_{COOH} is the carboxyl content of cellulose sample (mmol/g), C_{NaOH} and V_{NaOH} are the

molarity of NaOH and volume of NaOH (mL), respectively, C_{HCl} and V_{HCl} are the molarity of HCl and volume of HCl (mL), respectively, and m_{cell} is the mass of cellulose (g).

Liberation of carboxylic groups with an alkaline solution

To liberate the function of carboxylic groups and to achieve a better chelating function for the cations, carboxylated cellulose powder was poured into a beaker of distilled water and stirred rigorously and constantly for an hour. The pH of the suspension was measured and indicated an acidity of 3, as it contained cellulose with carboxylate functional groups. Later, the suspension was added with several drops of alkali solution made of 0.1 M NaOH to achieve a neutral pH. Subsequently, the modified cellulose was filtered and washed with distilled water and then oven dried. Finally, the dried carboxylated cellulose was ground into powder and kept in an airtight container to prevent moisture from being adsorbed from the surroundings. The reaction of neutralization of carboxylated cellulose with NaOH solution is as follows:

$$Cell - COOH + NaOH \rightarrow Cell - COONa + H_2O \quad \text{(Eq. 3)}$$

Preparation of metal ion and dye solutions

Three stock solutions of the metal ions Cu^{2+}, Pb^{2+}, and Cd^{2+} were obtained from Merck standard solution containing 1000 ppm of $Cu(NO_3)_2$, $Pb(NO_3)_2$, and $Cd(NO_3)_2$ in 0.5 M HNO_3 of the respective metal ions. Different concentrations were achieved via dilution with distilled water. Since the pH of the stock solution was very acidic, pH modification to reach near neutrality (close to 6) was achieved by adding an alkaline solution containing 0.1 M NaOH in distilled water. Meanwhile, the dye solution of methylene blue (MB) was prepared by pouring 1 g of MB into 1 L of distilled water in a volumetric flask to obtain a 1000 ppm concentration. Later, the stock solution was successively diluted with distilled water to obtain different concentrations of MB.

Metal ion and dye adsorption experiment

Metal ion adsorption tests were conducted using OPEFB-derived carboxylated cellulose for some aqueous contaminants, such as cationic metals, i.e., Cu^{2+}, Cd^{2+} and Pb^{2+} and dye, i.e., methylene blue (MB). To determine the adsorption performance of the adsorbent towards Cu^{2+}, Cd^{2+} and Pb^{2+}, and MB, the adsorption time and initial concentration were performed.

Kinetics study of adsorption

The kinetic study of adsorption for metal ions and MB was performed at an initial concentration of the metal and dye solution of 100 ppm. The concentration of the sample solution was determined by analyzing the filtrate using atomic absorption spectroscopy (AAS) for metal adsorption, while MB concentration was determined using UV visible spectrophotometer at a wavelength of 665 nm. To perform the adsorption test, 50 mg of powder cellulose was added into a 50 mL solution containing metal ions Pb^{2+}, Cu^{2+}, and $Cd^{2+}$and MB of 100 ppm in another 100 mL beaker and then, the flasks were placed on a magnetic stirrer. The metal ion and MB concentration of the solution was measured after a specified time interval, from 0 to 180 minutes. The adsorption capacity of modified cellulose (mg/g) was calculated following Eq. 4 (Zhang *et al.*, 2017):

$$Q_c = \frac{C_0 - C_1}{M} V \quad \text{(Eq. 4)}$$

where C_0 and C_1 are the initial and equilibrium concentrations (mg/L), M and V are the mass of the adsorbent (g) and the volume of the solution (L), respectively.

The adsorption tests were performed at room temperature and near neutral (pH <6) conditions. The pH was adjusted by adding drops of aqueous 0.1 M NaOH and/or 0.1M HCl solution. The metal ion uptake capacities were measured as a function of time to determine the optimal contact times for the adsorption of Pb^{2+}, Cu^{2+}, and Cd^{2+} ions. The contact times in the present study were set from 0 to 180 minutes. While performing the experiments, several µL of the solution samples were withdrawn at pre-determined time intervals and analyzed for metal adsorption using a syringe nylon filter with a pore size of 0.22 µm. The adsorption tests were conducted using OPEFB-derived unmodified cellulose and carboxylated cellulose.

Study on adsorption isotherm

To determine the maximum adsorption capacity of unmodified and carboxylated cellulose, three different 100 mL glass beakers containing 50 mL solution 100 ppm of metal ions Pb^{2+}, Cu^{2+}, Cd^{2+} ions, and MB were placed on a magnetic stirrer. The pH of the solution was adjusted by adding several drops of NaOH or HCl solution to the desired value. Later, a certain amount of modified cellulose, i.e., 50, 100, 150, 200, and 250 mg was poured into the solution in a beaker with constant stirring at 300 rpm. The suspension was constantly stirred at room temperature and allowed to sit for 24 hours for the adsorption process to occur. At the end of the process, 0.1 mL of filtrate was taken for analysis using AAS to determine the metal ion and UV vis to determine the MB remaining in the sample. Later, the results were adjusted with several isotherm adsorption models, such as Langmuir, Freundlich, or Sips.

Solution concentration determination

Determination of metal ion concentration in an aqueous sample from the adsorption test was carried out using the APHA methods. The atomic absorption spectrophotometer was used to determine solution concentration after the adsorption study was conducted using cellulose. The liquid sample was taken about 0.1 mL using a syringe nylon filter 0.22 um and then diluted. Later, the liquid was acidified with nitric acid (HNO_3) to a pH of 2 to ensure that the metal was well dissolved. Sample concentration was determined using a standard calibration curve established prior to measurement. The concentration of metal ions Cd^{2+}, Pb^{2+}, and Cu^{2+} was determined at wavelengths 228.8 nm, 283.3, and 324.7 nm, flame using air acetylene (A-Ac). The stock solution 1000 mg/L was used as the standard solution for a standard curve. All sample solutions were prepared with distilled water.

RESULTS AND DISCUSSION

Characteristics of OPEFB-derived carboxylated cellulose

Figure 2 presents the SEM analysis of the morphological structure of OPEFB-derived unmodified cellulose (Un-cell), carboxylated (Ca-cell) cellulose, and mercerized & carboxylated cellulose (Me-ca-cell). Samples of Ca-cell were carboxylated using succinic anhydride (SA) for 4 hours without mercerization, while Me-ca-cell samples were both mercerized and further proceeded with carboxylation. All samples were clean following the dewaxing process to remove wax and oil from the raw OPEFB. It can be seen that the fiber structure of Me-ca-cell has a longer and slimmer structure which is attributed to the larger surface area due to the mercerization process. The average fiber diameter of both Ca-cell and Me-ca-cell is 10 μm, and the fiber length is approximately 50 μm, indicating that the cellulose synthesized in this study is micro-cellulose.

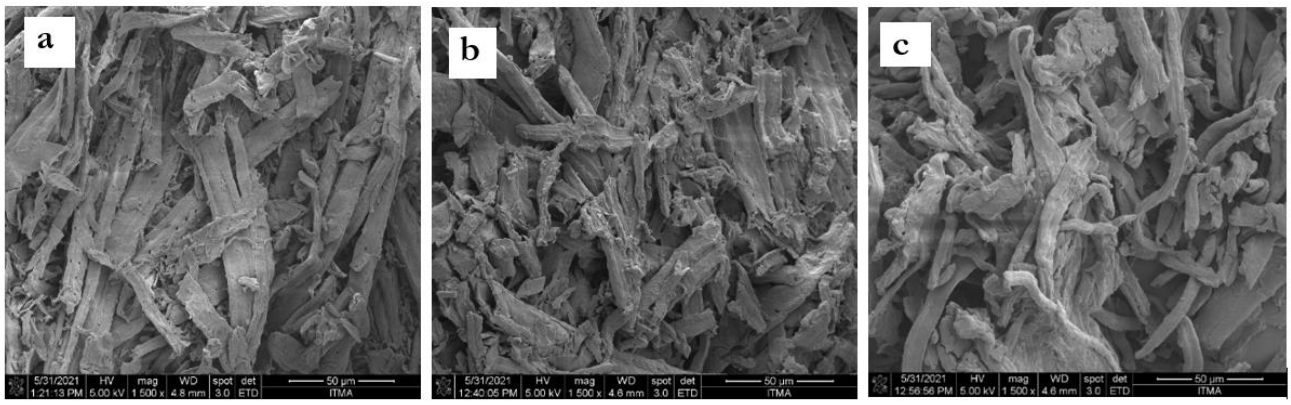

Figure 2. SEM images of (a) unmodified, (b) carboxylated (Ca-cell), and (c) mercerized & carboxylated (Me-ca-cell) OPEFB-derived cellulose

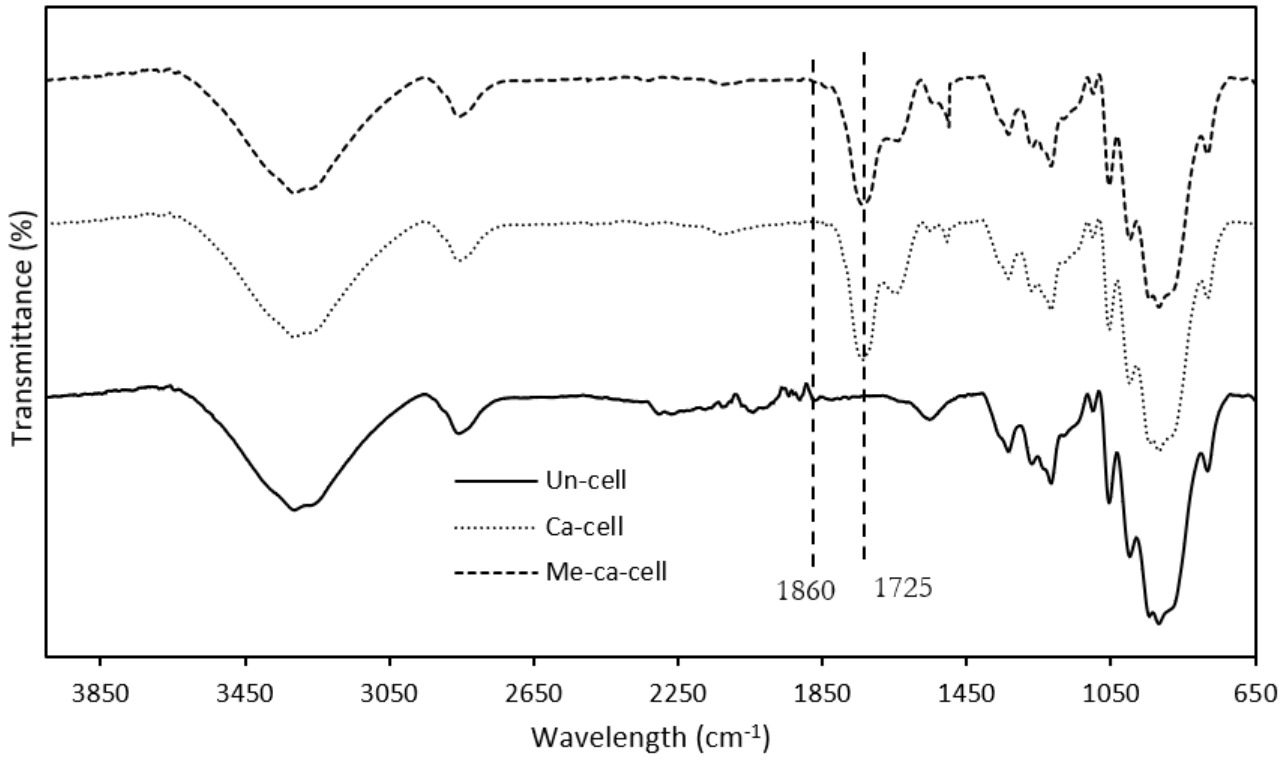

Figure 3. FTIR spectra of unmodified, carboxylated (Car-SA), and carboxylated and mercerized (CarMer-SA) OPEFB-derived cellulose

The FTIR analysis of unmodified cellulose, Ca-cell, and Me-ca-cell is presented in Figure 3. The partial carboxylation of the carboxylated cellulose hydroxyl groups was evidenced on FTIR spectra by the presence of the new band (stretching vibration) at 1725 cm^{-1} to 1735 cm^{-1} indicating C=O (carbonyl groups) stretching vibrations in ester bonds (Fan *et al.*, 2019; Leszczyńska *et al.*, 2019; Qiao *et al.*, 2015). Meanwhile, the band at the wavelengths 1860 and 1790 cm^{-1} is characterized SA (Leszczyńska *et al.*, 2019). Thus, the absence of carboxyl peak (−COOH) in these regions indicates that the samples are free from unreacted SA.

Furthermore, 2905 cm^{-1} assigns to the C-H vibration of -CH_2 groups is also evidenced in all samples. Meanwhile, there is a broad peak between 3200 and 3600 cm^{-1} related to -OH stretching. In both carboxylated cellulose samples (Ca-cell and Me-ca-cell), the intensity in this region changes due to the partial substitution of hydroxyl groups by carboxyl. The intensity of the band at 900 cm^{-1} increases after the mercerization step, which can be explained by the changes in the crystalline structure of cellulose-I to II (Astruc *et al.*, 2017).

The XRD analysis of the samples is shown in Figure 4a. A characteristic band between 13° and 17° and a broad peak at 22.5° are observed in the diffractogram, corresponding to cellulose-I. These results agree with those observed for native cellulose. These peaks are located at 2θ = 14°, 16°, 22.5° and arise from the crystallographic planes (101), (101) and (002), respectively. Importantly, a slight loss of crystallinity from the raw fibers to the mercerized cellulose is observed. This may be due to the conversion of cellulose-I to type-II (Me-ca-cell) (Astruc *et al.*, 2017; Gurgel *et al.*, 2008). Furthermore, they reported that mercerization reduces cellulose crystallinity.

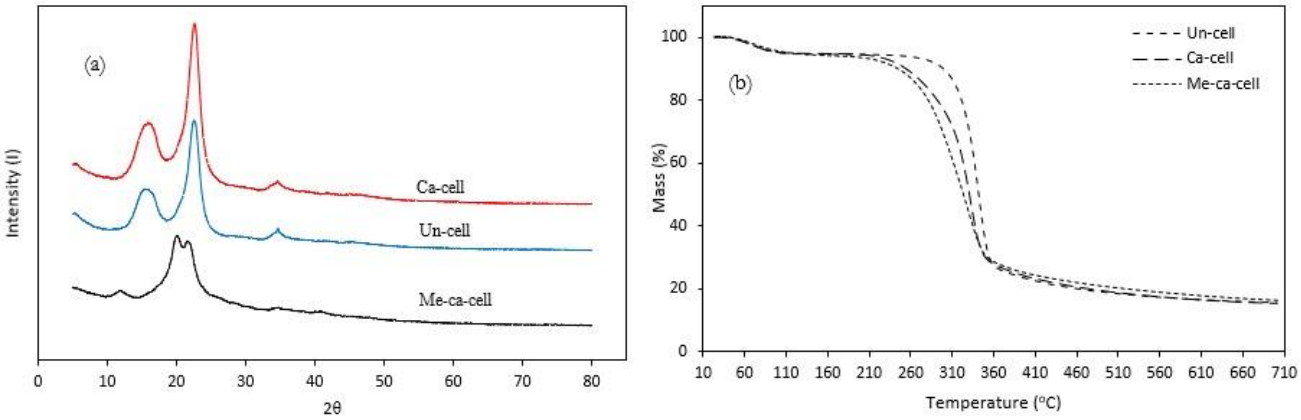

Figure 4. Diffractogram (a), and thermogram (b) of different types of cellulose

From Table 1, we can observe that crystallinity index of samples before mercerization (unmodified or native cellulose (un-cell) and carboxylated cellulose (Ca-cell) exhibit index of crystallinity of about 53.8 to 57.7%. However, after cellulose was mercerized (Me-ca-cell), its crystallinity value significantly decreased to 28.6% from unmodified OPEFB cellulose. Likewise, when mercerized cellulose was carboxylated (sample Me-ca-cell), its crystallinity also notably decreased to 28.2%. These findings are in line with other previous results revealing that mercerization can decrease degree of crystallinity of native cellulose (cellulose I) (Astruc *et al.,* 2017; Gurgel *et al.*, 2008).

Table 1. Crystallinity index of different samples of cellulose

2θ	Sample			
	Cell	**Ce**	**Me-cell**	**Me-ca-cell**
17	5950.99	7663.27	2963.07	4062.91
22	12888.04	18147.96	4147.63	5658.78
CI	0.54	0.58	0.28	0.28

The thermal properties of unmodified cellulose (un-cell), Ca-cell, and Me-ca-cell were compared to investigate their thermal stability. The TGA thermogram in Figure 4b shows that the Ca-cell has inferior thermal properties (T_0 and T_{max}) than the unmodified cellulose (pristine cellulose). The T_0 and T_{max} of unmodified are 270 and 364 °C, respectively, while the T_0 and T_{max} of Me-ca-cell are 208 and 349 °C. The results are in good agreement with Fan *et al.* (2019), Zhang *et al.* (2016), and Sehaqui *et al.* (2017), who demonstrated that samples with high carboxyl groups thermally decomposed at lower temperatures in comparison with pristine cellulose. The COOH functional group is much more unstable than the hydroxyl group in the native cellulose. Therefore, the higher content of this functional group will lower its thermal stability.

Carboxyl content of carboxylated cellulose

The carboxyl content of the carboxylated cellulose (Ca-cell and Me-ca-cell) was determined using the retro titration method. In general, as seen in Figure 5, the carboxyl content of all samples increases with reaction time from 1 to 4 hours. Overall, Me-ca-cell produced higher carboxyl content for all reaction times than the carboxylated cellulose without mercerization (Ca-cell). There is a significant increase in carboxyl content from 1 to 3 hours, indicating that there are still plenty of hydroxyl groups available to anchor carboxyl groups. However, the increase is less significant from 3 to 4 hours, indicating that the substitution of hydroxyl with carboxyl groups almost reached saturation. The high value of carboxyl content in Me-ca-cell cellulose is attributed to the carboxylation reaction between mercerized cellulose with SA. After a 4-hour reaction time, Me-ca-cell had the highest carboxyl content of 4.4 mmol/g, whereas Ca-cell had a carboxyl content of 1.8 mmol/g.

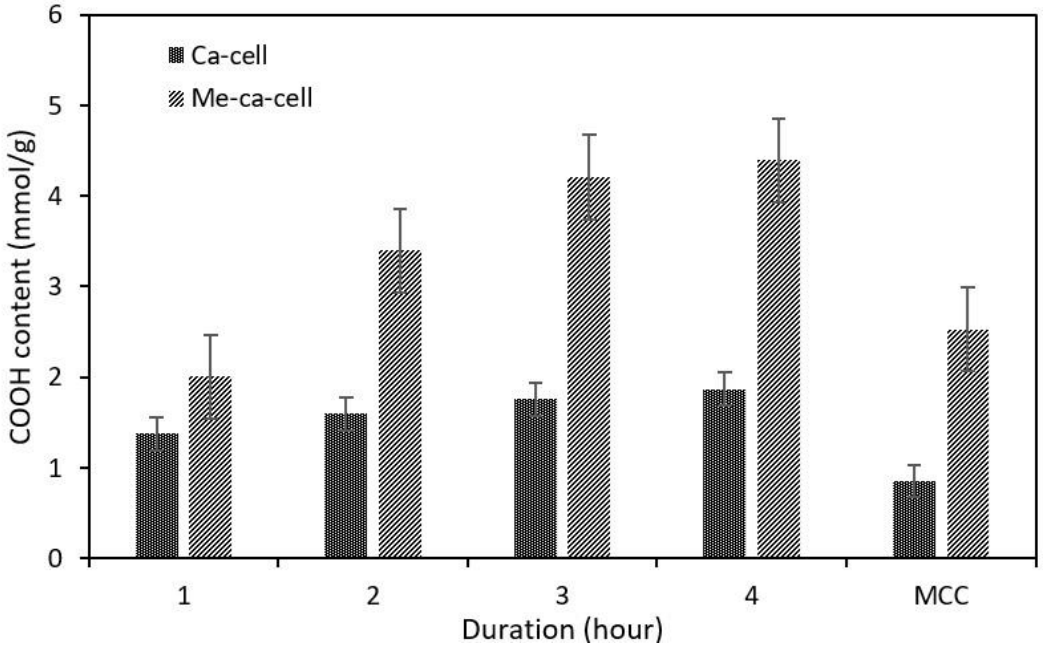

Figure 5. Carboxyl content of carboxylated cellulose

Compared to other studies, we found that using reagent SA can lead to cellulose production with higher carboxyl contents. Fan *et al.* (2019) synthesized cellulose nanocrystals modified with Fe^{2+}/H_2O_2 without mercerization and obtained the maximum carboxyl content of 2.2 mmol/g after 6 hours reaction time. In another study, Qiao et al. (2015) and Sehaqui *et al.* (2017b) determined the maximum carboxyl content of synthesized cellulose to be 3.4 mmol/g and 3.8 mmol/g, using reagents maleic anhydride and succinic anhydride, respectively, which is lower than the value obtained in this study. In a different study, Gurgel *et al.* (2008) determined that non-mercerized and mercerized cellulose contained 3.4 and 6.2 mmol/g of carboxyl, respectively. However, this might be due to the prolonged reaction time of 24 hours under pyridine reflux. Furthermore, the detailed comparison between the findings in this study with other studies is presented in Table 2.

Table 2. Comparison of carboxyl content in different protocols

Cellulose feedstock	Reagent/modification protocol	COOH content (mmol/g)	References
Commercial microcrystalline celluloses	Fe^{2+}/H_2O_2 oxidation	2.2	Fan *et al.*, 2019
Commercial cellulose	Maleic anhydride	3.4	Qiao *et al.*, 2015
Cellulose paper	Succinic anhydride in pyridine reflux	6.2	Gurgel *et al.*, 2008
Wheat fibers	Succinic anhydride	3.8	Sehaqui *et al.*, 2017
Commercial cellulose	Sodium 2-bromomalonate (BMA)	0.27	Gago *et al.*, 2020
OPEFB-derived Me-ca-cell	Succinic anhydride (SA)	4.4	This study

Heavy metals and dye adsorption

This kinetics study conducted the adsorption of three metal cations and methylene blue (MB) as a cationic dye for 180 minutes. Two different cellulose samples were used, i.e., Un-cell and Me-ca-cell, which reflects the performance of the two functional groups (hydroxyl and carboxyl groups) in binding metal cations. Sampling was carried out at a certain time interval, and the filtrate was analyzed to determine the sample metal cation and MB concentration. As metal cations of Pb^{2+}, Cu^{2+}, and Cd^{2+} precipitate at a solution pH above 6, the adsorption tests were performed at pH near 6 to achieve optimum metal ion adsorption.

For all metal cations, the results in Figure 6a to Figure 6b showed that Me-ca-cell has a considerably higher adsorption rate than unmodified cellulose (Un-cell). Me-ca-cell removed 97.85% of Pb^{2+} from the solution with the initial concentration of 100 ppm Pb^{2+} in distilled water after 180 min. On the other hand, Un-cell could only remove 23.1% of the metal cation from the same solution. Fig. 7 (b) also shows that the adsorption rate reached equilibrium at around 30 minutes. The trend is comparable for Cu^{2+} adsorption, although the maximum removal for this metal cation is much lower than Pb^{2+}. After being adsorbed by Me-ca-cell, Cu^{2+} concentration at the end of the adsorption process was only 51%. For Un-cell, the adsorption rate was much lower, accounting only for 2.9% removal. The adsorption process of metal cation Cd^{2+} after 180 min of adsorption time showed nearly 90.15% of Cd^{2+} removal by Ca-cell. In contrast, only 7.5% was removed by Un-cell.

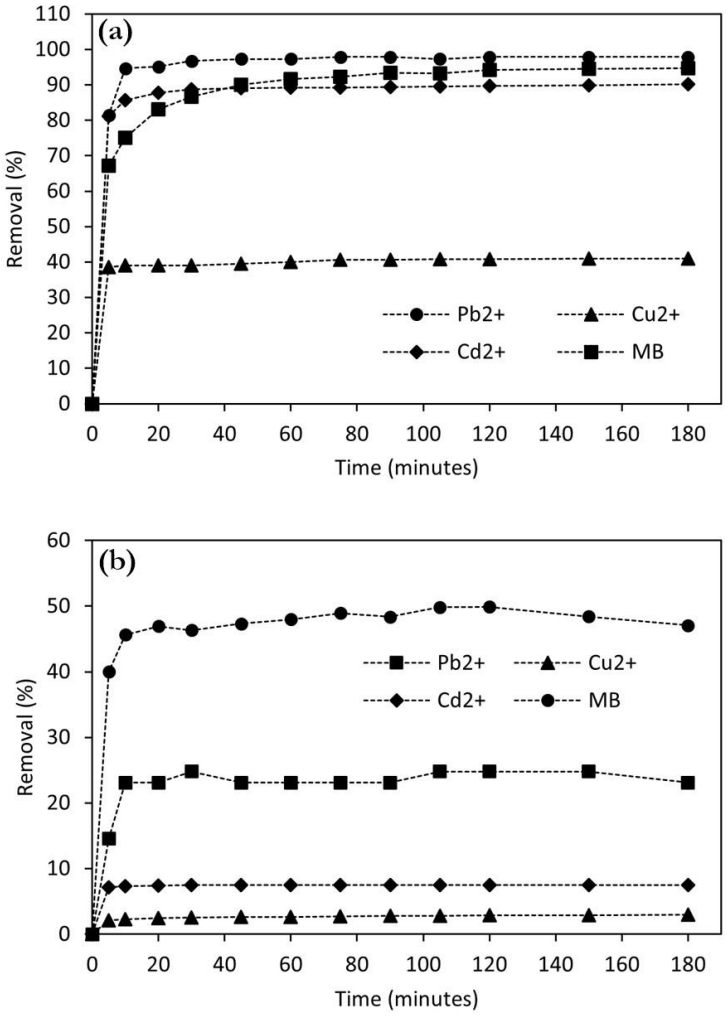

Figure 6. Removal rate of $Pb^{2+}Cu^{2+}$, Cd^{2+}, and MB of adsorbent of Me-ca-cell (a) and unmodified cellulose (b) at pH near neutral (~6)

In comparison, Diao *et al.* (2020) reported that the optimum adsorption of MB using cellulose-based adsorbent occurs below 10 min. However, we found that the curve reached a plateau after 60 min, indicating that the adsorption process had reached its maximum capacity. The maximum adsorption value of Me-ca-cell is 94.7 mg/g, or 94.7% removal, with Ca-cell having the highest adsorption rate compared to unmodified cellulose, recorded at 180 minutes. The longer optimum adsorption time might be due to the acidic nature of carboxyl cellulose, which impedes the adsorption of cationic dye. Nevertheless, these experimental results demonstrate that carboxyl functional groups in carboxylated cellulose have a higher metal and cationic dye-binding capacity than the hydroxyl groups of unmodified cellulose. Therefore, it is essential to customize the functional groups of native cellulose with more beneficial groups for adsorption purposes.

Adsorption kinetics

In order to identify the mechanism of dye and metal cations adsorption onto OPEFB-derived adsorbent, pseudo-first and second order of adsorption kinetics models were fitted with experimental data of different initial MB and metal cations concentrations. The adsorption duration was 180 minutes at pH near 6 using carboxylated cellulose as the adsorbent. Results in Figure 7 show that the pseudo-second order of adsorption kinetics fits well with the experimental data for MB and metal cations adsorption processes. The coefficients of determination are near unity. The regression equations and coefficient of determination values are also displayed in the figure. Meanwhile, the pseudo-first order does not fit with the experimental data.

Interaction between adsorbate and adsorbent is attributed to electrostatic interaction between cations (positively charged species, represented by metal and MB cations) and anions (negatively charged species, represented by carboxylated cellulose). Moreover, since the carboxylated functional groups on the cellulose previously reacted with NaOH to form COONa, the reaction to bind cations can be regarded as an ion exchange phenomenon as the presence of Na^+ is substituted by other cations. A previous study by Kowanga *et al.* (2016) obtained comparable results from an adsorption experiment of Pb^{2+} and Cu^{2+} on *Moringa oleifera* seed powder adsorbent. Al-Shannag *et al.* (2017) also discovered that metal Cd^{2+} removal by *Ballota undulata* biomass followed pseudo-second order of adsorption kinetics. In addition, the spontaneous exothermic nature of the adsorption indicated its feasibility for industrial applications. Generally, our findings show that the adsorption most likely occurs due to the chemisorption rather than the physisorption process, as also indicated by the aforementioned studies.

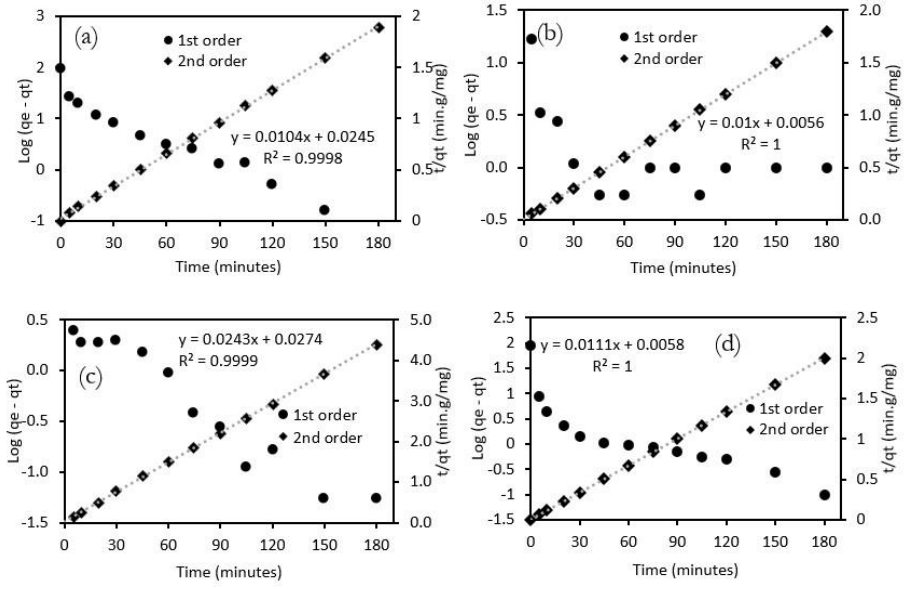

Figure 7. Pseudo-first and second order kinetics adsorption of methylene blue (a), Pb^{2+}(b), Cu^{2+}(c) , and Cd^{2+}(d)

Maximum adsorption test

The maximum adsorption of OPEFB-derived mercerized-carboxylated cellulose (Me-ca-cell) was carried out at pH near 6 for 24 hours while the suspension was rigorously and constantly stirred, and the results are presented in Figure 8. The initial concentration of the adsorbate was 100 mg/L. The maximum adsorption capacity of Me-ca-cell was found to be 98.5, 37.9, 68.5 and 99.5 mg/g for ion Pb^{2+}, Cu^{2+}, Cd^{2+}, and MB, respectively. Meanwhile, Un-cell only adsorbed those metal cations at the maximum range of 8.5, 2.9, 7.5 and 63 mg/g, respectively, which is significantly lower than Me-ca-cell. The findings revealed that the modification of cellulose with carboxylation and mercerization had higher adsorption capacities to three metal cations than unmodified cellulose.

In comparison, Wong *et al.* (2020) determined that the optimum conditions for Cu^{2+} adsorption from synthetic wastewater onto modified OPEFB adsorbent was at pH 5, initial concentration of 200 mg/L, and adsorbent dosage of 0.55 mg per 200 mL, contact time of 2.5 hours, yielding 52.5% of copper removal. Furthermore, using commercial activated carbon, Kavand *et al.* (2014) found that the optimum condition for Pb^{2+} and Cd^{2+} removal from wastewater treatment was at pH 7, at the initial concentration of metal ion 100 mg/L, an adsorbent dosage of 2 g/L, and contact time 80 minutes with Taguchi methodology for optimization parameter. Meanwhile, Javadian *et al.* (2015) conducted a study on the adsorption of Cd^{2+} from an aqueous solution using zeolite-based geopolymer (ZFA). They used synthesized adsorbent from coal fly ash. Based on their findings, the optimum adsorption conditions were at a ZFA dose of 0.08 g in 25 mL of Cd^{2+}, a contact time of 7 hours and pH 5.

Moreover, the metal adsorption mechanism is greatly pH-dependent, where Ge *et al.* (2017) found that the metal ion Cu^{2+} adsorption could be effectively performed at higher pH, for example, at initial pH 5. However, the removal efficiency of the metal ions decreased significantly when pH was lowered. It is because the excess proton in lower pH competes with metal ions to occupy active adsorbent sites. At the same time, active sites (carboxyl groups) of adsorbent are protonated at such a condition, carrying positive charges, providing repulsive action to cationic ions, such as Cu^{2+}. On the other hand, carboxylic groups are deprotonated at higher pH, providing active sites for the adsorption of cationic metal ions. However, at higher pH, metal ions tend to precipitate and form metal hydroxide, such as $Pb(OH)_2$, $Cu(OH)_2$, and $Cd(OH)_2$, which is insoluble in water (Kalak *et al.*, 2021).

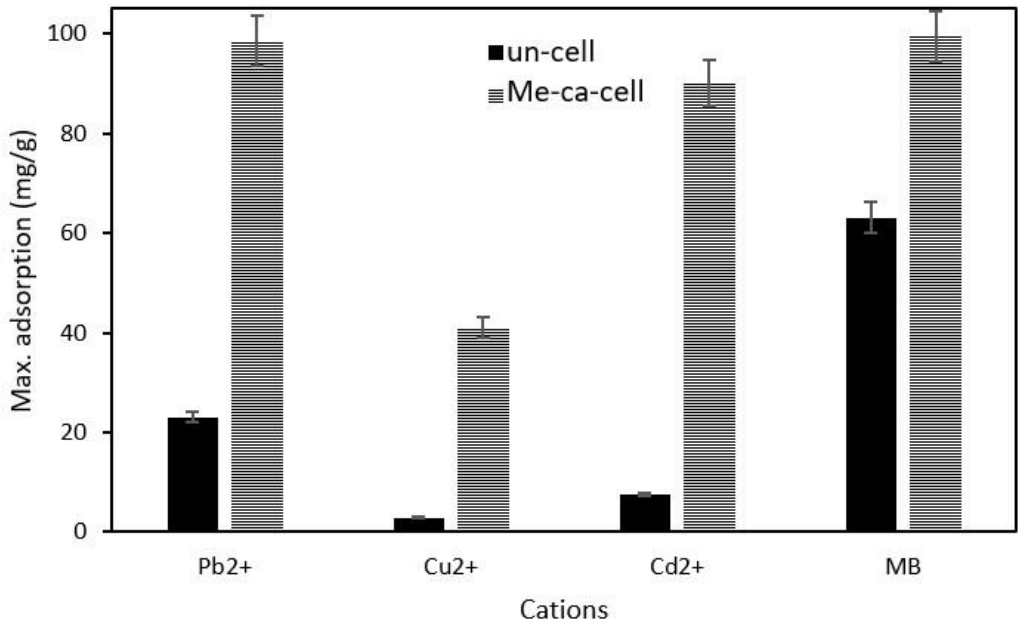

Figure 8. The maximum adsorption capacity of Me-ca-cell and unmodified cellulose (un-cell) toward metal ions and MB

The previous findings also revealed that the adsorption capacity for metal ion Pb^{2+} is higher than that of Cd^{2+}. For instance, Daochalermwong *et al.* (2020) found that the adsorption capacity of carboxylmethyl cellulose for Pb^{2+} and Cd^{2+} were 63.4 and 23.0 mg/g, respectively. They used cellulose adsorbent extracted from pineapple leaves and modified using ethylenediaminetetraacetic acid (EDTA) and carboxymethyl (CM) groups. In another study, Kalak *et al.* (2021b) conducted a study on the adsorption of sunflower wood fly ash toward two species of metal cations, Pb^{2+} and Cu^{2+}. They also reported that their synthesized adsorbent from agricultural residue has almost similar adsorption capacity to Pb^{2+} compared to Cu^{2+}, i.e., 32.94 mg/g (100 mg/L) to 32.70 mg/g (100 mg/L) with removal efficiency 99.81% and 99.61%, for Pb^{2+} and Cu^{2+} respectively. However, Xue *et al.* (2014) previously conducted an adsorption study using a similar adsorbent to several heavy metal cations and proved that the adsorption capacity/removal efficiency of their adsorbent follows the order: Pb^{2+}> Cd^{2+}>Cu^{2+}, i.e., 59.24, 55.37, and 32.82%, for Pb^{2+}, Cd^{2+}, and Cu^{2+}, which agrees with the results of this present study. This result is also in agreement with a previous study conducted by (Gurgel et al., 2008), in which they found that the adsorption of 30.4 mg/g, 86 mg/g, and 205.9 mg/g for Cu^{2+}, Cd^{2+} and Pb^{2+} respectively, using carboxylated cellulose adsorbent.

In comparison, the study conducted by Hariani *et al.* (2019) on modified cellulose via acetylation using acetic acid derivatized into cellulose-acetate as adsorbent found maximum of adsorption capacity of their synthesized cellulose acetate of 36.752 mg/g at initial concentration of MB 90 ppm, which is lower than this study. Another study on methylene blue removal was conducted by Kara *et al.* (2021). They synthesized nanocellulose from water hyacinth (Eichhornia crassipes) prepared using sodium periodate and found a removal efficiency of 90.91 mg/g.

From Table 3, it is noticeable that adsorption capacity to metal cations is further enhanced with the grafting with amino functional groups onto carboxylated cellulose as found in the study results conducted by Zhang *et al.* (2017), which account for 217.3 and 357.1 mg/g for Cd^{2+} and Pb^{2+}, respectively. They mentioned that the carboxyl and amino group content of their modified cellulose were 4.64 mmol/g and 2.61 mmol/g, respectively. The combination of these different functional groups grafted onto cellulose surface could enhance its adsorption capacity toward these two metal cations.

Table 3. Comparison on the maximum adsorption capacity of several adsorbents to metal cations

No	Adsorbent	Max. adsorption capacity (Qmax)	References
1	Adsorbent derived from municipal solid waste incineration fly ash	59.24, 55.37, and 32.82%, for Pb^{2+}, Cd^{2+}, and Cu^{2+}	Xue *et al.*, 2014
2	Aminopropyl- triethoxysilane (APS)/ microfibrillated cellulose (MFC) adsorbent	3.150 and 4.195 mmol/g for Cu^{2+} and Cd^{2+}	Hokkanen *et al.*, 2014
3	Carboxylated cellulose	30.4, 86.0, and 205.9 mg/g for Cu^{2+} Cd^{2+}, and Pb^{2+}	Gurgel *et al.,* 2008
4	Carboxymethyl cellulose	63.4 and 23.0 mg/g for Pb^{2+} and Cd^{2+}	Daochalermwong *et al.*, 2020
5	Carboxylated cellulose nanocrystals	465.1 mg/g, 344.8 m/g for Pb^{2+} and Cd^{2+}	Yu *et al.,* 2013
6	Carboxylated cellulose	217.3 and 357.1 mg/g for Cd^{2+} and Pb^{2+}	Zhang *et al.,* 2017
7	Carboxylated OPEFB cellulose	98.5 mg, 37.9, and 68.5 mg/g for ion Pb^{2+}, Cu^{2+}, and Cd^{2+}	This study

From the previous study findings, it revealed that adsorption capacity of cellulose for metal ion Pb^{2+} is higher than that of Cd^{2+}, which agrees with this study findings. For instance, Daochalermwong *et al.* (2020) revealed that the cellulose CM (carboxylmethyl) adsorption capacity for Pb^{2+} and Cd^{2+} accounted for 63.4 and 23.0 mg/g, respectively. In their study, they used cellulose adsorbent synthesized from pineapple leaves with modification using ethylenediaminetetraacetic acid (EDTA) and carboxymethyl (CM) groups. Furthermore, Xue *et al.* (2014) previously conducted an adsorption study using similar adsorbent to several heavy metal cations, proved that the adsorption capacity/removal efficiency of their adsorbent follows the order: Pb^{2+}> Cd^{2+}>Cu^{2+}, i.e., 59.24, 55.37, and 32.82%, for Pb^{2+}, Cd^{2+}, and Cu^{2+}, which agrees with the results of this present study (Table 2). This result is also in agreement with a previous study conducted by Gurgel *et al.* (2008) using carboxylated cellulose adsorbent, in which they found that the adsorption for Cu^{2+}, Cd^{2+} and Pb^{2+} were at 30.4 mg/g, 86 mg/g, and 205.9 mg/g respectively. In addition, the study results of Lim *et al.* (2019) found that adsorption capacity for Pb, Cd, and Cu at pH around 5 were 570.2–594.6, 302–311, and 126–144.5 mg/g, respectively using composite mineral adsorbent. However, they found that the adsorption capacity for Cd tended to decrease as the pH increased to 6.5 while that of Cu tended to increase as the pH increased to 6.5. Ali *et al.* (2017) found that maximum adsorption of Pb^{2+}, Cd^{2+} and Cu^{2+} were 91.5%, 90.18% and 75.08% for the dose of 0.4g/50 mL for lead and 0.6g/50mL for cadmium and copper using wheat straw as the adsorbent (see Table 4 below to observe the order of metal cation removal below based on various studies). In another study, Kalak *et al.* (2021) conducted a study on adsorption of sunflower wood fly ash toward two species of metal cations, Pb^{2+} and Cu^{2+}. They also reported that their synthesized adsorbent from agricultural residue has almost similar adsorption capacity to Pb^{2+} compared to Cu^{2+}, i.e., 32.94 mg/g (100 mg/L) to 32.70 mg/g (100 mg/L) with removal efficiency 99.81% and 99.61%, for Pb^{2+} and Cu^{2+} respectively.

The adsorption capacity of carboxylated cellulose toward Pb^{2+} is higher than that to Cu^{2+} and Cd^{2+}. It is also worth mentioning that Pb^{2+} has a higher electronegativity than Cd^{2+} and Cu^{2+}, which favor its higher adsorption efficiency, a better exchange with a sodium ion, thereby forming a better ionic bond. For instance, the electronegativity values for Pb^{2+}, Cd^{2+} and Cu^{2+} are 2.33, 1.69 and 1.9 respectively (Daochalermwong *et al.,* 2020). However, this explanation is inconsistent with some results (see Table 3 for comparison). If this is the case, the order of maximum adsorption capacity follows the order Pb^{2+}> Cu^{2+} > Cd^{2+}.

Table 4. Order of adsorption for several metal cations from various studies

Order of adsorption	Adsorption capacity and adsorbent used	Reference
Pb^{2+} > Cd^{2+} >Cu^{2+}	59.24, 55.37, and 32.82%, solid waste incineration fly ash	Xue *et al.,* 2014
	205.9, 86 30.4 mg/g, carboxylated cellulose	Gurgel *et al.,* 2008
	570.2–594.6, 302–311, and 126–144.5 mg/g, composite mineral	Lim *et al.,* 2019
	91.5%, 90.18% and 75.08%, wheat straw	Ali *et al.,* 2017
	- , 76.80, 72.10 mg/g, aminated *D. bipinnata*	Kour *et al.,* 2013
	589.32, 563.55, 81.7 mg/g, alkali-modified biochar from ginkgo leaves	Wang *et al.,* 2021
Pb^{2+}> Cu^{2+} >Cd^{2+}	66.7, 45.4, and 40.0 mg/g, Mesembryanthemum AC	Alkherraz *et al.,* 2020
	74.07, 69.93 and 60.24 mg/g, zeolite ZSM-5	Priyadi *et al.,* 2016
Cu^{2+}> Cd^{2+} >Pb^{2+}	83, 68, 52 mg/g, guanyl-modified cellulose (Gu-MC)	Kenawy *et al.,* 2018
	90.25, 55.23, and 35.12 mg/g silica functionalized with pyridin-2- ylmethanol (SiPy)	Tighadouini *et al.,* 2021

According to Yu *et al.* (2013), a larger ionic radius reduces the electrostatic nature of a metal ion. In term of charge density, Pb, Cd, and Cu have the value of 32, 59, and 116, C/mm^3, respectively (Rayner-Canham, 1976). In addition, Pb^{2+} adsorption was favorable in the system since its smaller hydrated radius (4.01 Å) and lower pKH (7.71), ensuring for adsorption through inner surface complexation than two other metal cations (Wang *et al.*, 2021).

There is evidence of complexation of three metal ions after adsorption with C=C group, indicating M^{2+} -π bond. Meanwhile, the adsorption of Cu was due to the main mechanism of its complexation with specific functional groups. The order of metal ion adsorption depends on the adsorbent characteristics. Thus, different adsorbent has different order of maximum value of metal ion adsorption (Wang *et al.*, 2021).

Adsorption isotherm

Isotherm studies were conducted to describe how OPEFB-derived carboxylated cellulose interacts with adsorbates by correlation of equilibrium data. Two models of adsorption isotherm, i.e., Langmuir and Freundlich, were fitted with the data obtained from the experiments in this study. The Langmuir adsorption isotherm assumes that adsorption of sorbate takes place in one layer of molecule in thickness on the surface of the sorbent. Meanwhile, the Freundlich isotherm assumes a heterogeneous surface with a multilayer of molecules adsorbate over the adsorbent surface.

The analyses were performed for three metal cations, i.e. Pb^{2+}, Cu^{2+}, and Cd^{2+}. Five doses of CarMer-SA cellulose were dispersed in a solution containing 100 mg/L (100 ppm) metal ions. The experimental results of this study were plotted linearly with both Langmuir and Freundlich isotherm models. The results in Figure 9a to Figure 9h show that both models fit well with the experimental data. For the lead (Pb^{2+}) adsorption test, the Langmuir model is better fitted (Figure 9a, 9b) since its coefficient of determination value is greater than that of Freundlich's. Therefore, we assume the lead adsorption process satisfies the Langmuir model.

Nonetheless, for the adsorption process of copper (Cu^{2+}), the Freundlich model fits better due to its higher value of determination coefficient than that of Langmuir's (Figure 9c, 9d). Therefore, it is concluded that the copper adsorption process follows the Freundlich isotherm model. In the Langmuir model, ions are assumed to be adsorbed as a monolayer on the adsorbent surface. Thus, the adsorption process reaches a maximum when its surface is completely covered by adsorbate. Meanwhile, Freundlich assumes that adsorbent has heterogeneous surfaces and multilayer adsorption with different affinities (Sun & Selim, 2020).

Moreover, the experimental data for cadmium (Cd^{2+}) were fitted with two models of adsorption isotherm like previous methods. The results are compared in Figure 9e, 9f. Both isotherm models fitted well with the experimental data, indicating by the coefficient of determination value (R^2) was greater than 0.9. However, by observing the R^2 value of both models, we conclude that the Langmuir model with a higher R^2 value better fits with the experimental data of the cadmium adsorption process in this study.

Furthermore, as shown in Figure 9g, 9h, the adsorption procedure for MB using CarMer-SA cellulose fits both the Freundlich and Langmuir models. Langmuir model is better fitted with the adsorption process since the R^2 value is slightly higher than the other model. The current study results are slightly different from that of (Gago *et al.*, 2020) that found under an acidic environment (pH 3), the MB adsorption isotherms fitted the Langmuir isotherm model with a maximum value of the capacity reaching 887.6 mg/g. Furthermore, at pH near neutral (pH around 6.4), the model that best fits the adsorption process is the Sips model, which generated S-shape curves.

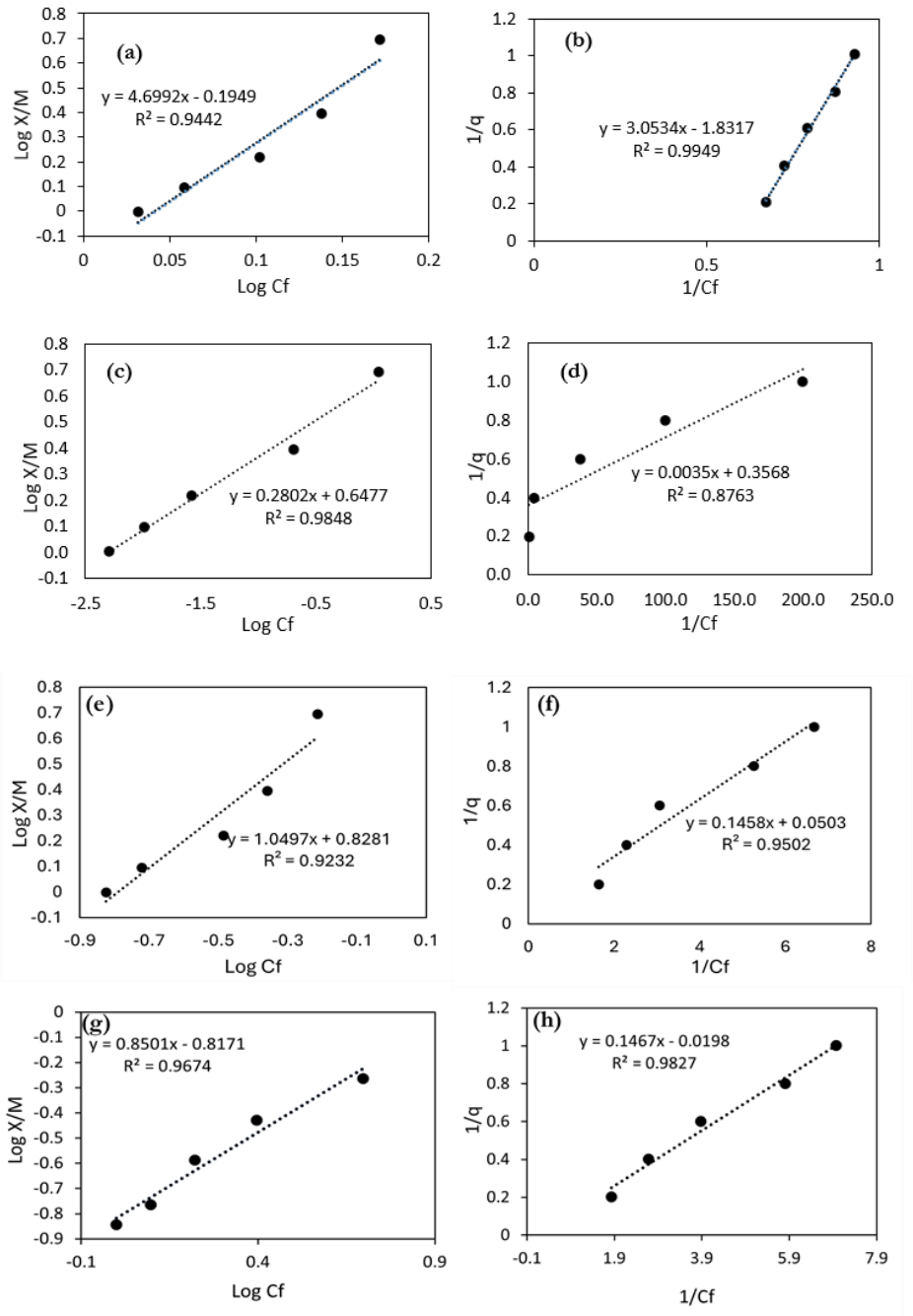

Figure 9. Adsorption isotherm of Pb^{2+} to CarMer-SA; (a) Freundlich and (b) Langmuir model; Cu^{2+} to CarMer-SA: Freundlich (c), and Langmuir model (d); Cd^{2+} to CarMer-SA: Freundlich (e) and Langmuir model (f); MB to CarMer-SA: Freundlich (g), and Langmuir model (h)

CONCLUSION

This study produced potential bioadsorbents for metal cations and dyes from oil palm empty fruit bunches (OPEFB) by modifying OPEFB-derived cellulose with succinic anhydride (SA) via carboxylation with pyridine as a catalyst. The results showed that the carboxylation reaction using SA enabled the substitution of native hydroxyl groups with the carboxyl groups, enhancing the adsorption capacity and metal-binding capability of OPEFB-derived cellulose. The characterization of the modified cellulose

indicated that the cellulose synthesized in this study is micro-cellulose with significant characteristics of the ester and carboxyl functional groups. The maximum carboxyl content produced after a 4-hr reaction time was 4.2 mmol/g. This study also found that the mercerization process of cellulose prior to the functional group modification increased the carboxyl content.

The adsorption performance of carboxylated mercerized cellulose was found to have higher adsorption capacity than that of unmodified cellulose with 98.5, 37.9, 68.5 and 99.5 mg/g for ion Pb^{2+}, Cu^{2+}, Cd^{2+}, and MB, respectively at pH~6. The adsorption processes better fit the pseudo-second-order model, indicating that the adsorption process is most likely caused by chemisorption rather than physisorption. According to batch isotherm tests, the heavy metal cations and MB, except for Cu^{2+}, were adsorbed as a monolayer onto the cellulose surface. Thus, the adsorption process reaches a maximum when its surface is completely covered by adsorbate. Our research revealed that carboxylated OPEFB cellulose with SA can be considered as an eco-friendly and cost-effective sorbent for metal cations and dyes in aquatic media. Based on our findings and previous research, we can conclude that OPEFB-derived carboxylated cellulose is an excellent adsorbent for metal cations and dyes.

ACKNOWLEDGEMENTS

We would like to acknowledge SEARCA (Southeast Asian Regional Center for Graduate Study and Research in Agriculture) and Universiti Putra Malaysia for providing the research grant for this study: UPM.IKP.800-2/2/22/Matching (6390100).

CONFLICT OF INTEREST

The authors have declared that no conflict of interest exists.

REFERENCES

Al-Shannag, M., Al-Qodah, Z., Nawasreh, M., Al-Hamamreh, Z., Bani-Melhem, K., & Alkasrawi, M. 2017. On the performance of ballota undulata biomass for the removal of cadmium(II) ions from water. *Desalination and Water Treatment* 67(April): 223. https://doi.org/10.5004/dwt.2017.20379

Alkherraz, A. M., Ali, A. K., & Elsherif, K. M. 2020. Equilibrium and thermodynamic studies of Pb(II), Zn(II), Cu(II) and Cd(II) adsorption onto mesembryanthemum activated carbon. *Journal of Medicinal and Chemical Sciences* 3(1): 1–10. https://doi.org/10.26655/JMCHEMSCI.2020.1.1

Asadpour, R., Yavari, S., Kamyab, H., Ashokkumar, V., Chelliapan, S., & Yuzir, A. 2021. Study of oil sorption behaviour of esterified oil palm empty fruit bunch (OPEFB) fibre and its kinetics and isotherm studies. *Environmental Technology & Innovation* 22: 101397. https://doi.org/https://doi.org/10.1016/j.eti.2021.101397

Astruc, J., Nagalakshmaiah, M., Laroche, G., Grandbois, M., Elkoun, S., & Robert, M. 2017. Isolation of cellulose-II nanospheres from flax stems and their physical and morphological properties. *Carbohydrate Polymers* 178(August): 352–359. https://doi.org/10.1016/j.carbpol.2017.08.138

Awalludin, M. F., Sulaiman, O., Hashim, R., & Nadhari, W. N. A. W. 2015. An overview of the oil palm industry in Malaysia and its waste utilization through thermochemical conversion, specifically via liquefaction. *Renewable and Sustainable Energy Reviews* 50: 1469–1484. https://doi.org/10.1016/j.rser.2015.05.085

Bhadoria, P., Shrivastava, M., Khandelwal, A., Das, R., Langyan, S., Rohatgi, B., & Singh, R. 2022. Preparation of modified rice straw-based bio-adsorbents for the improved removal of heavy metals from wastewater. *Sustainable Chemistry and Pharmacy* 29: 100742. https://doi.org/https://doi.org/10.1016/j.scp.2022.100742

Ching, Y. C., & Ng, T. S. 2014. Effect of preparation conditions on cellulose from oil palm empty fruit bunch fiber. *BioResources* 9(4): 6373–6385. https://doi.org/10.15376/biores.9.4.6373-6385

Chong, W. C., Choo, Y. L., Koo, C. H., Pang, Y. L., & Lai, S. O. 2019. Adsorptive membranes for heavy metal removal - A mini review. *AIP Conference Proceedings* 2157(September). https://doi.org/10.1063/1.5126540

Daneshfozoun, S, Abdullah, M. A., & Abdullah, B. 2017. Preparation and characterization of magnetic biosorbent based on oil palm empty fruit bunch fibers, cellulose and Ceiba pentandra for heavy metal ions removal. *Industrial Crops and Products* 105: 93–103. https://doi.org/https://doi.org/10.1016/j.indcrop.2017.05.011

Daneshfozoun, Safoura, Nazir, M. S., Abdullah, B., & Abdullah, M. A. 2014. Surface modification of celluloses extracted from oil palm empty fruit bunches for heavy metal sorption. *Chemical Engineering Transactions* 37(May): 679–684. https://doi.org/10.3303/CET1437114

Daochalermwong, A., Chanka, N., Songsrirote, K., Dittanet, P., Niamnuy, C., & Seubsai, A. 2020. Removal of Heavy Metal Ions Using Modified Celluloses Prepared from Pineapple Leaf Fiber. *ACS Applied Materials and Interfaces*. https://doi.org/10.1021/acsomega.9b04326

Diao, H., Zhang, Z., Liu, Y., Song, Z., Zhou, L., Duan, Y., & Zhang, J. 2020. Facile fabrication of carboxylated cellulose nanocrystal–MnO2 beads for high-efficiency removal of methylene blue. *Cellulose* 27(12): 7053–7066. https://doi.org/10.1007/s10570-020-03260-0

Fan, X. M., Yu, H. Y., Wang, D. C., Mao, Z. H., Yao, J., & Tam, K. C. 2019. Facile and Green Synthesis of Carboxylated Cellulose Nanocrystals as Efficient Adsorbents in Wastewater Treatments. *ACS Sustainable Chemistry and Engineering* 7(21): 18067–18075. https://doi.org/10.1021/acssuschemeng.9b05081

Gago, D., Chagas, R., Ferreira, L. M., Coelhoso, I., & Velizarov, S. 2020. A Novel Cellulose-Based Polymer for Efficient Removal of Methylene Blue. *Membranes* 10(13): 1–17.

Ge, Y., Cui, X., Liao, C., & Li, Z. 2017. Facile fabrication of green geopolymer/alginate hybrid spheres for efficient removal of Cu(II) in water: Batch and column studies. *Chemical Engineering Journal* 311(Ii): 126–134. https://doi.org/10.1016/j.cej.2016.11.079

Gurgel, L. V. A., Júnior, O. K., Gil, R. P. de F., & Gil, L. F. 2008. Adsorption of Cu(II), Cd(II), and Pb(II) from aqueous single metal solutions by cellulose and mercerized cellulose chemically modified with succinic anhydride. *Bioresource Technology* 99(8): 3077–3083. https://doi.org/10.1016/j.biortech.2007.05.072

Hariani, P. L., Riyanti, F., & Kurniaty, A. 2019. Modification of cellulose with acetic acid to removal of methylene blue dye. *Journal of Physics: Conference Series* 1282(1). https://doi.org/10.1088/1742-6596/1282/1/012079

Hokkanen, S., Repo, E., & Sillanpää, M. 2013. Removal of heavy metals from aqueous solutions by succinic anhydride modified mercerized nanocellulose. *Chemical Engineering Journal* 223: 40–47. https://doi.org/10.1016/j.cej.2013.02.054

Hokkanen, S., Repo, E., Suopajärvi, T., Liimatainen, H., Niinimaa, J., & Sillanpää, M. 2014. Adsorption of Ni(II), Cu(II) and Cd(II) from aqueous solutions by amino modified nanostructured microfibrillated cellulose. *Cellulose* 21(3): 1471–1487. https://doi.org/10.1007/s10570-014-0240-4

Javadian, H., Ghorbani, F., Tayebi, H. allah, & Asl, S. M. H. 2015. Study of the adsorption of Cd (II) from aqueous solution using zeolite-based geopolymer, synthesized from coal fly ash; kinetic, isotherm and thermodynamic studies. *Arabian Journal of Chemistry* 8(6): 837–849. https://doi.org/10.1016/j.arabjc.2013.02.018

Kalak, T., Cierpiszewski, R., & Ulewicz, M. 2021. High efficiency of the removal process of pb(Ii) and cu(ii) ions with the use of fly ash from incineration of sunflower and wood waste using the cfbc technology. *Energies* 14(6). https://doi.org/10.3390/en14061771

Kara, H. T., Anshebo, S. T., Sabir, F. K., & Adam Workineh, G. 2021. Removal of Methylene Blue Dye from Wastewater Using Periodiated Modified Nanocellulose. *International Journal of Chemical Engineering* 2021. https://doi.org/10.1155/2021/9965452

Kassab, Z., Syafri, E., Tamraoui, Y., Hannache, H., Qaiss, A. E. K., Achaby], M. [El, & El Achaby, M. 2019. Characteristics of sulfated and carboxylated cellulose nanocrystals extracted from Juncus plant stems. *International Journal of Biological Macromolecules* 154. https://doi.org/https://doi.org/10.1016/j.ijbiomac.2019.11.023

Kassab, Z., Syafri, E., Tamraoui, Y., Hannache, H., Qaiss, A. E. K., & El Achaby, M. 2020. Characteristics of sulfated and carboxylated cellulose nanocrystals extracted from Juncus plant stems. *International Journal of Biological Macromolecules* 154: 1419–1425. https://doi.org/10.1016/j.ijbiomac.2019.11.023

Kavand, M., Kaghazchi, T., & Soleimani, M. 2014. Optimization of parameters for competitive adsorption of heavy metal ions (Pb+2, Ni+2, Cd+2) onto activated carbon. *Korean Journal of Chemical Engineering* 31(4): 692–700. https://doi.org/10.1007/s11814-013-0280-8

Kenawy, I. M., Hafez, M. A. H., Ismail, M. A., & Hashem, M. A. 2018. Adsorption of Cu(II), Cd(II), Hg(II), Pb(II) and Zn(II) from aqueous single metal solutions by guanyl-modified cellulose. *International Journal of Biological Macromolecules* 107: 1538–1549. https://doi.org/10.1016/j.ijbiomac.2017.10.017

Kour, J., Homagai, P. L., Cagnin, M., Masi, A., Pokhrel, M. R., & Ghimire, K. N. 2013. Adsorption of Cd (II), Cu (II), and Zn (II) from Aqueous Solution onto Nitrogen-Functionalized Desmostachya bipinnata. *Journal of Chemistry* 2013. https://doi.org/10.1155/2013/649142

Kowanga, K. D., Mauti, G. O., Mauti, E. M., & Gatebe, E. 2016. Kinetic, sorption isotherms, pseudo-first-order model and pseudo-second-order model studies of Cu(II) and Pb(II) using defatted Moringa oleifera seed powder. *The Journal of Phytopharmacology* 5(2): 71–78. www.phytopharmajournal.com

Le, N. L., & Nunes, S. P. 2016. Materials and membrane technologies for water and energy sustainability. *Sustainable Materials and Technologies* 7: 1–28. https://doi.org/10.1016/j.susmat.2016.02.001

Lee, H. V., Hamid, S. B. A., & Zain, S. K. 2014. Conversion of lignocellulosic biomass to nanocellulose: Structure and chemical process. *Scientific World Journal* 2014(August 2014). https://doi.org/10.1155/2014/631013

León, O., Muñoz-Bonilla, A., Soto, D., Pérez, D., Rangel, M., Colina, M., & Fernández-García, M. 2018. Removal of anionic and cationic dyes with bioadsorbent oxidized chitosans. *Carbohydrate Polymers* 194: 375–383. https://doi.org/10.1016/j.carbpol.2018.04.072

Leszczyńska, A., Radzik, P., Szefer, E., Mičušík, M., Omastová, M., & Pielichowski, K. 2019. Surface modification of cellulose nanocrystals with succinic anhydride. *Polymers* 11(5). https://doi.org/10.3390/polym11050866

Lim, W. R., Kim, S. W., Lee, C. H., Choi, E. K., Oh, M. H., Seo, S. N., Park, H. J., & Hamm, S. Y. 2019. Performance of composite mineral adsorbents for removing Cu, Cd, and Pb ions from polluted water. *Scientific Reports* 9(1): 1–10. https://doi.org/10.1038/s41598-019-49857-9

Moradi, O., Pudineh, A., & Sedaghat, S. 2022. Synthesis and characterization Agar/GO/ZnO NPs nanocomposite for removal of methylene blue and methyl orange as azo dyes from food industrial effluents. *Food and Chemical Toxicology* 169(August): 113412. https://doi.org/10.1016/j.fct.2022.113412

Priyadi, ., Iskandar, ., Suwardi, ., & Mukti, R. R. 2016. Characteristics of Heavy Metals Adsorption Cu, Pb and Cd Using Synthetics Zeolite Zsm-5. *Journal of Tropical Soils* 20(2): 77. https://doi.org/10.5400/jts.2015.v20i2.77-83

Qiao, H., Zhou, Y., Yu, F., Wang, E., Min, Y., Huang, Q., Pang, L., & Ma, T. 2015. Effective removal of cationic dyes using carboxylate-functionalized cellulose nanocrystals. *Chemosphere*, 141: 297–303. https://doi.org/10.1016/j.chemosphere.2015.07.078

Rayner-Canham. 1976. Charge Densities of Selected Ions. *Descriptive Inorganic Chemistry*: 13–15. https://bcs.whfreeman.com/WebPub/Chemistry/raynercanham6e/Appendices/Rayner-Canham 5e Appendix 2 - Charge Densities of Selected Ions.pdf

SefidSiahbandi, M., Moradi, O., Akbari –adergani, B., Azar, P. A., & Tehrani, M. S. 2023. Fabrication and implementation of bimetallic Fe/Zn nanoparticles (mole ratio 1:1) loading on hydroxyethylcellulose – Graphene oxide for removal of tetracycline antibiotic from aqueous solution. *Chemosphere* 312(P1): 137184. https://doi.org/10.1016/j.chemosphere.2022.137184

Sehaqui, H., Kulasinski, K., Pfenninger, N., Zimmermann, T., & Tingaut, P. 2017. Highly Carboxylated Cellulose Nanofibers via Succinic Anhydride Esterification of Wheat Fibers and

Facile Mechanical Disintegration. *Biomacromolecules* 18(1): 242–248. https://doi.org/10.1021/acs.biomac.6b01548

Septevani, A. A., Afandi, F. R., Sampora, Y., Septiyanti, M., Devy, Y. A., Amelia, A. R., & Burhani, D. 2020. Solely Cellulose-based Adsorbent Derived from Oil Palm Empty Fruit Bunches for Dye Removal. *Reaktor; Volume 20 No.3 September 2020DO - 10.14710/Reaktor.20.3.122-128* . https://ejournal.undip.ac.id/index.php/reaktor/article/view/29348

Sjahro, N., Yunus, R., Abdullah, L. C., Rashid, S. A., Asis, A. J., & Akhlisah, Z. N. 2021. Recent advances in the application of cellulose derivatives for removal of contaminants from aquatic environments. In *Cellulose* (Vol. 28, Issue 12). Springer Netherlands. https://doi.org/10.1007/s10570-021-03985-6

Song, S., Liu, Z., Zhang, J., Jiao, C., Ding, L., & Yang, S. 2020. Synthesis and Adsorption Properties of Novel Bacterial Cellulose / Graphene Oxide / Attapulgite. *Materials* 13: 3703.

Suhas, Gupta, V. K., Carrott, P. J. M., Singh, R., Chaudhary, M., & Kushwaha, S. 2016. Cellulose: A review as natural, modified and activated carbon adsorbent. *Bioresource Technology* 216: 1066–1076. https://doi.org/10.1016/j.biortech.2016.05.106

Sun, W., & Selim, H. M. 2020. *Chapter Two - Fate and transport of molybdenum in soils: Kinetic modeling* (D. L. B. T.-A. in A. Sparks (ed.); Vol. 164, pp. 51–92). Academic Press. https://doi.org/10.1016/bs.agron.2020.06.002

Tighadouini, S., Radi, S., Roby, O., Hammoudan, I., Saddik, R., Garcia, Y., Almarhoon, Z. M., & Mabkhot, Y. N. 2021. Kinetics, thermodynamics, equilibrium, surface modelling, and atomic absorption analysis of selective Cu(ii) removal from aqueous solutions and rivers water using silica-2-(pyridin-2-ylmethoxy)ethan-1-ol hybrid material. *RSC Advances* 12(1): 611–625. https://doi.org/10.1039/d1ra06640d

Wang, D., Luo, W., Zhu, J., Wang, T., Gong, Z., & Fan, M. 2021. Potential of removing Pb, Cd, and Cu from aqueous solutions using a novel modified ginkgo leaves biochar by simply one-step pyrolysis. *Biomass Conversion and Biorefinery* 0123456789. https://doi.org/10.1007/s13399-021-01732-2

Wong, H. W., Ibrahim, N., Hanif, M. A., Noor, N. M., Yusuf, S. Y., & Hasan, M. 2020. Optimization of copper adsorption from synthetic wastewater by oil palm-based adsorbent using Central Composite Design. *IOP Conference Series: Earth and Environmental Science* 476(1). https://doi.org/10.1088/1755-1315/476/1/012104

Xue, Q., Li, J. S., Wang, P., Liu, L., & Li, Z. Z. 2014. Removal of heavy metals from landfill leachate using municipal solid waste incineration fly ash as adsorbent. *Clean - Soil, Air, Water* 42(11): 1626–1631. https://doi.org/10.1002/clen.201300619

Yang, H., Zhang, X., Luo, H., Liu, B., Shiga, T. M., Li, X., Kim, J. I., Rubinelli, P., Overton, J. C., Subramanyam, V., Cooper, B. R., Mo, H., Abu-Omar, M. M., Chapple, C., Donohoe, B. S., Makowski, L., Mosier, N. S., McCann, M. C., Carpita, N. C., & Meilan, R. 2019. Overcoming cellulose recalcitrance in woody biomass for the lignin-first biorefinery. *Biotechnology for Biofuels* 12(1): 1–18. https://doi.org/10.1186/s13068-019-1503-y

Yu, X., Tong, S., Ge, M., Wu, L., Zuo, J., Cao, C., & Song, W. 2013. Adsorption of heavy metal ions from aqueous solution by carboxylated cellulose nanocrystals. *Journal of Environmental Sciences (China)* 25(5): 933–943. https://doi.org/10.1016/S1001-0742(12)60145-4

Zhang, C., Su, J., Zhu, H., Xiong, J., Liu, X., Li, D., Chen, Y., & Li, Y. 2017. The removal of heavy metal ions from aqueous solutions by amine functionalized cellulose pretreated with microwave-H2O2. *RSC Advances* 7(54): 34182–34191. https://doi.org/10.1039/c7ra03056h

Zhang, K., Sun, P., Liu, H., Shang, S., Song, J., & Wang, D. 2016. Extraction and comparison of carboxylated cellulose nanocrystals from bleached sugarcane bagasse pulp using two different oxidation methods. *Carbohydrate Polymers* 138: 237–243. https://doi.org/10.1016/j.carbpol.2015.11.038

Zhou, H., Zhu, H., Xue, F., He, H., & Wang, S. 2020. Cellulose-based amphoteric adsorbent for the complete removal of low-level heavy metal ions via a specialization and cooperation mechanism. *Chemical Engineering Journal* 385(December 2019): 123879. https://doi.org/10.1016/j.cej.2019.123879

Zulfiqar Ali, S., Athar, M., Salman, M., & Imran Din, M. 2017. Simultaneous removal of Pb(II), Cd(II) and Cu(II) from aqueous solutions by adsorption on Triticum aestivum - a green approach. *Hydrology: Current Research 02*(04): 4–11. https://doi.org/10.4172/2157-7587.1000118